

Computer-aided Quantification of Pulmonary Fibrosis in Patients with Lung Cancer: Relationship to Disease-free Survival

Tae Iwasawa, MD, PhD • Koji Okudela, MD, PhD • Tamiko Takemura, MD, PhD • Taiki Fukuda, MD • Shoichiro Matsushita, MD, PhD • Tomohisa Baba, MD • Takashi Ogura, MD, PhD • Michihiko Tajiri, MD, PhD • Atsuko Yoshizawa

From the Departments of Radiology (T.I., T.F., S.M.), Respiratory Medicine (T.B., T.O.), and Thoracic Surgery (M.T.), Kanagawa Cardiovascular and Respiratory Center, 6-16-1, Tomioka-higashi, Kanazawa-ku, Yokohama 236-8651, Japan, Kanagawa, Japan; Department of Pathology, Graduate School of Medicine, Yokohama City University, Kanagawa, Japan (K.O.); Department of Pathology, Japanese Red Cross Medical Center, Tokyo, Japan (T.T.); Department of Radiology, the Jikei University School of Medicine, Tokyo, Japan (T.F.); Department of Radiology, St Marianna University School of Medicine, Kanagawa, Japan (S.M.); and Department of Biostatistics and Epidemiology, Tokyo University of Science, Tokyo, Japan (A.Y.). Received October 24, 2018; revision requested December 17; final revision received March 17, 2019; accepted April 10. **Address correspondence to** T.I. (e-mail: tae_i_md@wb3.so-net.ne.jp).

Supported in part by Japan Society for the Promotion of Science KAKENHI (grant number 15K09901).

Conflicts of interest are listed at the end of this article.

See also the editorial by Goo in this issue.

Radiology 2019; 292:489–498 • <https://doi.org/10.1148/radiol.2019182466> • Content codes: **CH** **CT** **OI**

Background: Interstitial lung abnormalities (ILAs) are present at CT in about 10% of individuals undergoing lung cancer screening. The relationship between histologic findings of ILAs and their influence on patient prognosis remains unknown.

Purpose: To evaluate the percentage of ILAs at preoperative CT, as measured by radiologists and a computer-aided detection (CAD) software, as a predictor of disease-free survival in patients with lung cancer.

Materials and Methods: This retrospective study evaluated 217 consecutive patients who underwent complete resection of lung cancer from April 2010 to December 2015. Two radiologists, blinded to the patients' clinical information, scored percentage fibrosis extent and determined whether ILAs and the usual interstitial pneumonia (UIP) pattern were present. They assessed ILA progression at follow-up CT. Two pathologists determined the presence of an UIP pattern. Percentage fibrosis extent was also measured by using CAD. Binary logistic regression analysis was performed to determine whether the CAD percentage fibrosis extent was associated with ILA at CT. Multivariable Cox regression analysis was used to evaluate the significance of CAD percentage fibrosis extent as a predictor of prognosis.

Results: The radiologists classified 47 patients with ILAs and 24 patients with a UIP pattern at chest CT. The pathologists detected a UIP pattern in 25 patients. CT abnormalities showed progression over a 2-year period in all patients with histologic evidence of UIP. After adjustment for age, sex, and smoking index, the CAD percentage fibrosis extent was independently associated with ILA (odds ratio: 3.1; 95% confidence interval [CI]: 2.1, 4.7; $P < .001$). After adjustment for age, forced expiratory volume in 1 second (percentage predicted) radiologist-assessed percentage fibrosis extent, and pathologic stage, CAD percentage fibrosis extent was independently associated with worse disease-free survival (hazard ratio: 1.3; 95% CI: 1.1, 1.6; $P < .001$).

Conclusion: Greater computer-aided detection percentage fibrosis extent at preoperative CT independently predicted worse disease-free survival in patients with lung cancer.

© RSNA, 2019

Online supplemental material is available for this article.

There is increasing awareness of the clinical importance of incidentally detected interstitial lung abnormalities (ILAs) on non-contrast-enhanced chest CT images (1). Large cohort studies (2–5) of lung cancer screening have reported that ILAs are present in 8%–10% of participants. ILAs have been associated with a greater risk of all-cause mortality (1,2). Miller et al (6) recently reported that some subclinical ILAs at CT represent an early stage or a mild form of pulmonary fibrosis. Moreover, ILAs influence survival in patients with advanced lung cancer (7). Outcomes are reported to be poorer in patients with lung cancer with idiopathic pulmonary fibrosis (IPF) than in patients without IPF (8–10). However, quantitative evaluation of ILAs in patients with lung cancer and their influence on survival have not yet been fully investigated.

Many computer-aided detection (CAD) systems have been developed to quantify diffuse lung abnormalities at CT (11–14). Subpleural abnormalities at CT, as measured by using the Gaussian histogram normalized correlation (GHNC) system, correspond to a histologic usual interstitial pneumonia (UIP) pattern of fibrosis in patients with interstitial lung diseases (ILDs) (15).

Thus, we hypothesized that the volume of ILAs at CT measured using a GHNC-CAD system would be associated with the UIP CT pattern and worse prognosis in patients with lung cancer. The purpose of this study was to quantify ILAs at preoperative CT by using a GHNC-CAD system and to evaluate the extent of ILAs as a predictor of disease-free survival (DFS) in patients with lung cancer. We also evaluated the

This copy is for personal use only. To order printed copies, contact reprints@rsna.org

Abbreviations

CAD = computer-aided detection, CI = confidence interval, DFS = disease-free survival, GHNC = Gaussian histogram normalized correlation, ILA = interstitial lung abnormality, ILD = interstitial lung disease, IPF = idiopathic pulmonary fibrosis, OR = odds ratio, SRIF = smoking-related interstitial fibrosis, UIP = usual interstitial pneumonia

Summary

Greater pulmonary fibrosis percentage measured by computer-aided detection at preoperative CT is an independent predictor of worse disease-free survival in patients with lung cancer.

Key Points

- Of 217 patients with lung cancer, 47 (21.7%) had interstitial abnormalities at CT, which was associated with worse disease-free survival (hazard ratio [HR]: 3.3; $P < .001$); histologic specimens showed a usual interstitial pneumonia pattern in 25 patients (11.5%), and these CT abnormalities progressed at follow-up.
- The percentage of pulmonary fibrosis measured by computer-aided detection software was independently associated with interstitial abnormalities at CT (odds ratio: 3.1; $P < .001$).
- In adjusted models, the greater percentage of pulmonary fibrosis at CT measured by computer-aided detection software was independently associated with worse disease-free survival (HR: 1.3; $P < .001$).

histologic findings of ILAs and the progression of ILAs on follow-up CT images.

Materials and Methods

Patients

Our institutional review board approved this retrospective single-center study and waived the requirement for obtaining informed patient consent (KCRC-17-0051). Consecutive patients who underwent lung cancer surgery from April 2010 to December 2015 (see Appendix E1 [online]) in our hospital were potential candidates (Fig 1). Among 739 patients, we excluded patients who had previously undergone thoracic surgery ($n = 59$) or radiation therapy ($n = 2$) and patients who had previously had severe tuberculosis or other infectious diseases ($n = 8$) or interstitial pneumonia associated with collagen vascular disease ($n = 3$). We excluded 38 patients with pathologic stage III cancer ($n = 37$) or IV cancer ($n = 1$) (16), as well as 412 patients who had not undergone CT performed without contrast material in our hospital within 3 months before surgery. The final study population comprised 217 patients who underwent video-assisted thoracic surgery for lung cancer. Smoking status was determined by using medical records (7).

CT Evaluation by Radiologists

Presurgical thin-section volumetric CT images (1-mm sections) were obtained without contrast material at full inspiration (see Appendix E1 [online]).

Two expert chest radiologists (S.M. and T.F., each with 10 years of experience) independently evaluated preoperative CT images in random order without any clinical information. They scored the extent of each lesion, as reported previously (17), and we used the average of the two results. We calculated the sum of reticulation and honeycombing as the percentage fibrosis extent for each examination.

The radiologists evaluated whether ILAs existed by using a previously reported scoring system (3), where a score of 1 indicated no ILAs; a score of 2, equivocal ILAs; and a score of 3, ILAs. Figure 2 shows examples of the ILA severity grades. The radiologists then determined whether a UIP pattern was present on the basis of previously established criteria (18). A third radiologist (T.I., with 25 years of experience) who was blinded to the clinical information provided the majority opinion in cases of discrepant results between the first two radiologists.

The radiologists also evaluated the progression of ILAs at follow-up CT examinations at 1 year and 2 years, as reported previously (19). Determination of fibrosis progression was based on any increase in abnormal findings on the follow-up studies. CT images showing lung cancer recurrence were excluded from the analysis of follow-up CT studies.

CAD of Fibrosis Percentage

Analysis of preoperative CT images by using the GHNC-CAD system (Mebius, Yokohama, Japan) has been previously described in detail (15,20,21), and additional details are provided in Appendix E1 (online). The “H” pattern in the GHNC system includes honeycombing and fibrosis with traction bronchiectasis/bronchiolectasis. We measured H-pattern volume and expressed it as a percentage of the total CT lung volume. We defined this H-pattern volume ratio as the percentage fibrosis extent based on the GHNC system. We determined the subpleural lung area as the outer part of the lung within 2 mm deep to the visceral pleura and calculated the subpleural percentage fibrosis extent (according to the H2 pattern) with CAD (15).

Pathologic Analysis and Multidisciplinary Diagnosis

To analyze the histologic features of ILAs, two expert lung pathologists (T.T., with 35 years, and K.O., with 20 years of experience) evaluated the pathologic specimens to determine whether interstitial abnormalities were present on the basis of histologic criteria (22–25); see Appendix E1 (online) for details. One pulmonologist (T.B., with 20 years of experience), one radiologist (T.I.), and one pathologist (K.O.) discussed whether the patient had IPF, another type of ILD, or no ILD, on the basis of all data, including follow-up CT studies, according to previously established guidelines (21,25).

Statistical Analysis

Interobserver agreement between the two radiologists and between the two pathologists was assessed with weighted κ analysis. Interobserver agreement was classified as “slight” ($\kappa = 0.00$ – 0.20), “fair” ($\kappa = 0.21$ – 0.40), “moderate” ($\kappa = 0.41$ – 0.60), “good” ($\kappa = 0.61$ – 0.80), or “excellent” ($\kappa = 0.81$ – 1.00) (26). Interobserver agreement on percentage fibrosis extent between the two radiologists was analyzed by calculating intraclass correlation coefficients. We performed Pearson correlation analysis to determine the relationship between the extent of CT abnormalities determined by the radiologists and GHNC-CAD results. We identified clinical factors associated with the presence of ILAs with binary logistic regression analysis. Univariable and multivariable Cox proportional hazard models were used to

examine the significance of the clinical characteristics and CT findings of percentage fibrosis extent as predictors of DFS. Cumulative survival curves were constructed by using the Kaplan-Meier method. For this analysis, we determined the cutoff values of percentage fibrosis extent by using receiver operating characteristic curve analysis for the radiologists and the CAD system separately. These statistical analyses were performed by using SPSS, version 21 (IBM, Armonk, NY). The *Z* test for binomial proportion with continuity adjustment (performed by using SAS 9.4 M5 [SAS, Cary, NC]) showed that the sample size of 217 was sufficient to detect a 10% increase in computer reading, with power of about 90%. *P* < .05 was considered to indicate a significant difference.

Results

The final study population comprised 217 consecutive patients with pathologic stage Ia (*n* = 151), stage Ib (*n* = 47), stage IIa (*n* = 15), or stage IIb (*n* = 4) lung cancer. There were 136 men (mean age, 70.0 years ± 8.6 [standard deviation]; range, 36–86 years) and 81 women (mean age, 65.0 years ± 10.4; range, 36–86 years). The mean patient age was 68.2 years ± 9.6 (range, 36–86 years). Seventeen patients had a past medical history of an ILD diagnosis. No patients received any adjuvant or neoadjuvant therapy prior to surgical resection of their clinically limited lung cancer. Patients in this study cohort received chemotherapy and/or radiation therapy only after recurrence.

Table 1 summarizes the patient demographics and disease characteristics. One hundred forty (64.5%) patients were smokers. Median follow-up time was 1456 days (range, 20–2921 days). Lung cancer recurred in 29 patients, and a total of 32 patients died of any cause, including postoperative acute IPF exacerbation (Fig 3 and Table E1 [online]).

Table 2 summarizes the CT results. The median delay between preoperative CT and surgery was 41 days (range, 1–90 days).

Interobserver agreement between the two radiologists was moderate for pattern classification (κ = 0.6) (Appendix E1 [online]). Among the 217 included patients, the radiologists identified 143 (65.9%) patients without ILAs, 27 (12.4%) patients with equivocal ILAs, and 47 (21.7%) patients with ILAs. On the basis of consensus results, 24 (11.1%) patients showed the UIP CT pattern (there were concordant and discordant results for 16 and eight patients, respectively). The mean percentage fibrosis extent determined by the radiologists was 3.1% ± 6.3, and the intraclass correlation coefficient was 0.89 (Appendix E1 [online]).

Interobserver agreement between the pathologists was good (κ = 0.66) for histologic determination of UIP; the results for 19 and six patients were concordant and discordant, respectively. One pathologist considered discordant cases to represent smoking-related interstitial fibrosis (SRIF).

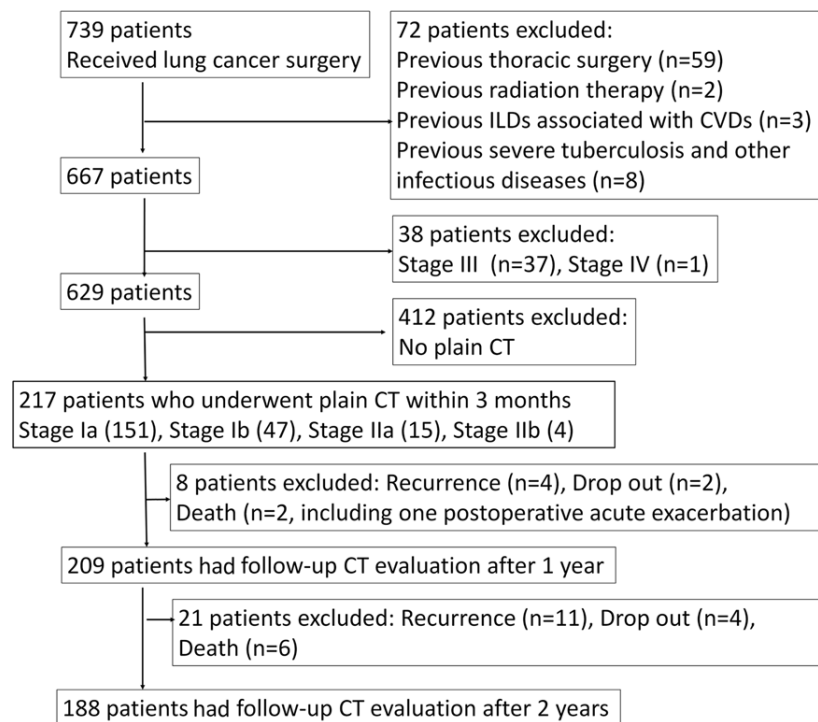


Figure 1: Flowchart of the selection of the study population and the exclusion criteria. CVD = collagen vascular disease, ILD = interstitial lung disease.

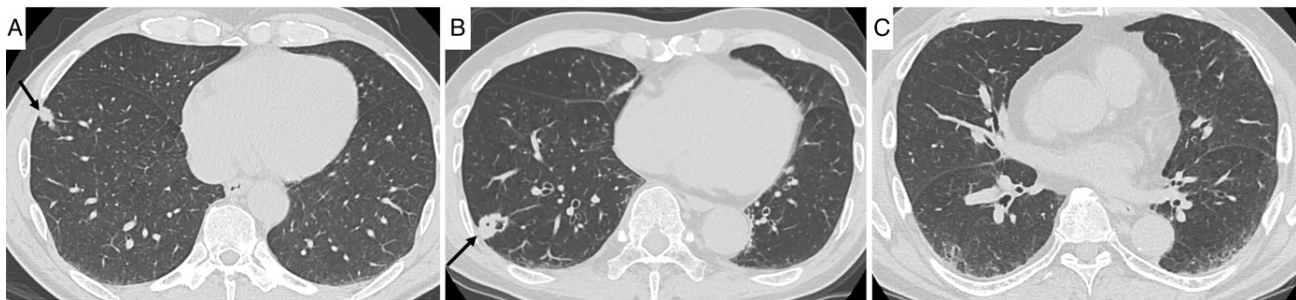


Figure 2: Axial CT images show the severity grades of interstitial lung abnormalities (ILAs). A, No ILAs. Arrow = lung cancer. B, Equivocal ILAs (reticulation < 5%) are present in the right lung base. Arrow = lung cancer. C, ILAs (reticulation > 5%) are present in the bilateral lung bases, which showed the usual interstitial pneumonia pattern in the histologic specimens.

Among the 217 patients, 25 (11.5%) had a histologic UIP pattern, 11 (5.1%) had ILD other than UIP (nonspecific interstitial pneumonia [$n = 3$] or unclassifiable interstitial pneumonia [$n = 8$]; Fig E1 [online]), 54 (24.9%) had SRIF, and 127 (58.5%) had no ILAs. All patients with a UIP CT pattern had some histologic interstitial abnormalities, and among the 25 patients with histologic UIP, 19 (76.0%) had a UIP CT pattern.

The radiologists analyzed 209 CT studies and 188 CT studies obtained after 1 year and 2 years, respectively. In 24 patients with the UIP CT pattern, ILAs clearly or possibly progressed in 86.3% of patients (19 of 22) and 94.4% of patients (17 of 18) after 1 year and 2 years, respectively (Fig 4). In 23 patients with ILAs other than the UIP pattern, ILAs clearly or possibly progressed in 50.0% of patients (11 of 22) after 1 year and in 65.0% of patients (13 of 20) after 2 years (Fig 4). No patient without ILAs at initial CT developed de novo ILAs during the follow-up period. In the 25 patients with histologic UIP, ILAs progressed in 81.8% of patients (18 of 22) after 1 year and in 100% of patients (20 of 20) after 2 years (Figs 4, 5).

Table 2 summarizes the CAD results. With CAD, the mean percentage fibrosis extent was $4.5\% \pm 2.8$, and the subpleural percentage fibrosis extent was $20.1\% \pm 9.0$. The percentage fibrosis extent according to GHNC correlated well with the fibrosis extent according to the radiologists (Pearson correlation coefficient = 0.88; $P < .001$; Table E2 [online]).

Multivariable binary logistic regression analysis identified age and smoking index as significant clinical factors associated with the presence of ILAs at CT and the UIP pattern at CT (Table E3 [online]). In multivariable binary logistic regression analysis, CAD percentage fibrosis extent was an independent predictor ($P < .001$) of the presence of ILAs (odds ratio [OR], 3.1; 95% confidence interval [CI]: 2.1, 4.7) or the UIP pattern at CT (OR, 2.0; 95% CI: 1.5, 2.6) after adjustment for age, sex, and smoking index (Table 3). After adjustment for age and smoking index, the extent of subpleural percentage fibrosis with CAD independently predicted a histologic UIP pattern (OR, 1.2; 95% CI: 1.1, 1.3; $P < .001$).

By using our multidisciplinary diagnostic approach, 25 (11.5%) patients were given a diagnosis of IPF; all had histologic UIP. Eleven (44%) of 25 patients with IPF died because of cancer recurrence ($n = 5$) or IPF ($n = 6$). However, one patient recovered from a bout of acute exacerbation 2 years after surgery and is currently cancer free (Fig 5).

Figure 6 shows Kaplan-Meier curves comparing DFS and histologic and radiologic parameters. Receiver operating characteristic curve analysis results are shown in Appendix E1, Figure E2, and Table E4 (all online). Log-rank tests revealed significant differences in survival probability between the two groups based on the percentage fibrosis extent determined by radiologists (fibrosis $\geq 7.5\%$ and fibrosis $< 7.5\%$, $P < .001$) and that determined by GHNC (H pattern $\geq 5.0\%$ and H pattern $< 5.0\%$, $P < .001$), as well as subpleural percentage fibrosis extent (H2 pattern $\geq 27\%$ and H2 pattern $< 27\%$, $P < .001$). The Kaplan-Meier curves comparing overall survival are shown in Figure E3 (online), and univariable and multivariable Cox regression analysis results are shown in Tables E5 and E6 (online).

Univariable Cox regression analysis results for each factor for predicting DFS are shown in Tables 1 and 2 and Table E1 (online). The existence of ILAs predicted poorer DFS (hazard ratio, 3.3; 95% CI: 1.8, 6.2; $P < .001$) (ie, more death from lung cancer). The presence of a UIP pattern at CT was a greater risk for DFS (hazard ratio, 5.3; 95% CI: 2.5, 11.1; $P < .001$), with comparisons between other groups as follows: no ILA versus control and equivocal ILA (hazard ratio, 1.8; 95% CI: 0.66, 4.9; $P = .25$) and ILA not UIP (hazard ratio, 2.4; 95% CI: 0.93, 6.0; $P = .072$).

A direct comparison between percentage fibrosis extent as determined by radiologists and that as determined by CAD is shown in Table E7 (online). Table 4 shows the multivariable Cox regression analysis results. After adjusting for age, forced expiratory volume in 1 second, maximum cancer diameter, the percentage fibrosis extent determined by radiologists, and lung cancer stage, we found that the GHNC-CAD percentage fibrosis extent remained associated with poorer DFS (hazard ratio, 1.3; 95% CI: 1.1, 1.6; $P = .001$ [Table 4]).

Discussion

We measured the extent of interstitial lung abnormalities (ILAs) on preoperative CT studies in patients with lung cancer as percentage fibrosis extent by means of a computer-aided detection (CAD) system employing Gaussian histogram normalized correlation (GHNC). A larger GHNC-based percentage fibrosis extent predicted the existence of ILAs (odds ratio [OR], 3.1; $P < .001$) and a usual interstitial pneumonia (UIP) pattern at CT (OR, 1.2; $P < .001$). Multivariable regression analysis showed that percentage fibrosis extent measured by CAD using GHNC significantly and independently predicted worse disease-free survival (DFS) (hazard ratio, 1.3; $P < .001$). UIP is a known risk factor for acute exacerbation in patients after lung cancer surgery, chemotherapy, and radiation therapy (27–31). We found that determining the percentage fibrosis extent with CAD was useful for evaluating the existence and severity of ILAs at preoperative CT and for risk stratification of patients with lung cancer.

Our hospital encounters more than 500 new patients with ILDs per year. Many patients with lung cancer are referred to our hospital because of associated ILDs, which explains the larger incidence of ILAs in our study group. When the 17 patients with a previous consultation history for ILDs were excluded, 30 (15.0%) of 200 patients had ILAs, which was not markedly different from previously reported frequencies: 24% reported by Kanaji et al (30), 23% reported by Sverzellati et al (31), and 14% reported by Nishino et al (7).

In the current study, CT findings in patients with histologic UIP showed progression over a period of 1–2 years: five patients died of respiratory failure. Moreover, acute exacerbation occurred in three patients, including one patient with mild ILAs. This suggests that mild ILAs in some patients are early evidence of pulmonary fibrosis (6,19). Our results indicate that careful follow-up is necessary for patients with lung cancer with a histologic UIP pattern in the surgical specimen, even when the initial CT findings are unremarkable, because these patients are at an increased risk for cancer recurrence and early death (32).

Table 1: Patient Characteristics and Their Associations with Disease-free Survival according to Univariable Cox Regression Analysis

Characteristic	Total (<i>n</i> = 217)	No ILA (<i>n</i> = 143 [65.9%])	Equivocal ILA (<i>n</i> = 27 [12.4%])	ILA (<i>n</i> = 47 [21.7%])		Disease-free Survival	
				Not UIP (<i>n</i> = 23 [10.6%])	UIP (<i>n</i> = 24 [11.1%])	Hazard Ratio*	<i>P</i> Value
Age (y) [†]	68.2 ± 9.6	66.5 ± 10.0	68.5 ± 9.7	72.6 ± 7.9	73.2 ± 5.2	1.1 (1.0, 1.1)	.001
Sex						8.6 (2.7, 28)	.001
No. of male patients	136 (62.7)	76 (53.1)	17 (67.0)	20 (87.0)	23 (95.8)		
No. of female patients	81 (37.3)	67 (46.9)	10 (37.0)	3 (13.0)	1 (0.4)		
History of smoking	140 (64.5)	79 (55.2)	18 (66.7)	19 (82.6)	24 (100)	3.5 (1.3, 8.9)	.01
Smoking index (no. of pack-years) [†]	28.7 ± 31.3	21.0 ± 27.8	27.5 ± 28.3	47.1 ± 34.7	58.5 ± 27.3	1.02 (1.02, 1.03)	<.001
Surgical procedure						2.1 (0.99, 4.4) [‡]	.051
Wedge resection	28 (12.9)	14 (9.8)	4 (14.8)	3 (13.0)	7 (29.2)		
Segmentectomy	17 (7.8)	14 (9.8)	0	0	3 (12.5)		
Lobectomy	172 (79.2)	115 (80.4)	23 (85.2)	20 (87.0)	14 (58.3)		
Pathologic stage						4.1 (1.9, 8.5) [§]	<.001
Ia	151 (69.6)	112 (78.3)	15 (55.6)	15 (65.2)	9 (37.5)		
Ib	47 (21.7)	22 (15.4)	7 (25.9)	6 (26.1)	12 (50.0)		
IIa	15 (6.9)	8 (5.6)	5 (18.5)	1 (4.3)	1 (4.2)		
IIb	4 (1.8)	1 (0.7)	0	1 (4.3)	2 (8.3)		
Maximum cancer diameter (mm) [†]	19.9 ± 11.1	18.3 ± 10.5	19.4 ± 11.9	21.2 ± 11.3	28.4 ± 10.3	1.04 (1.02, 1.07)	.002
Histologic finding						0.27 (0.15, 0.51)	<.001
Adenocarcinoma	174 (80.1)	130 (90.9)	23 (85.2)	8 (34.7)	13 (54.2)		
Squamous cell carcinoma	31 (13.3)	10 (7.0)	2 (7.4)	12 (52.2)	7 (29.2)		
Other	12 (5.5)	3 (2.1)	2 (7.4)	3 (13.0)	4 (16.7)		
FVC (%) [†]	104.5 ± 16.0	106.0 ± 15.9	110.1 ± 13.1	103.6 ± 13.9	90.7 ± 14.9	0.98 (0.96, 0.998)	.03
FEV ₁ (%) [†]	94.5 ± 21.5	96.6 ± 20.7	90.7 ± 21.2	95.4 ± 22.0	85.1 ± 23.7	0.98 (0.97, 0.99)	.003
FEV ₁ /FVC [†]	72.3 ± 11.9	72.2 ± 12.1	66.8 ± 11.6	73.0 ± 11.9	78.2 ± 7.7	0.99 (0.97, 1.0)	.578
MDD							
None	170 (78.3)	142 (99.3)	26 (96.3)	2 (8.7)	0	Control	
ILDs (not IPF)	22 (10.1)	1 (0.7)	1 (3.7)	15 (65.2)	5 (20.8)	3.1 (1.4, 7.0)	<.001
IPF	25 (11.5)	0	0	6 (26.1)	19 (11.5)	4.5 (2.1, 9.4)	<.001
Frequency of histologic findings							
Emphysema	148 (68.2)	90 (62.3)	17 (63.0)	19 (82.6)	22 (91.7)	4.6 (1.6, 13.0)	.004
Fibrosis	97 (44.7)	42 (29.4)	11 (40.7)	21 (91.3)	23 (95.8)	3.2 (1.6, 6.2)	.001
Subpleural fibrosis	37 (17.1)	3 (2.3)	4 (14.8)	10 (43.5)	19 (79.1)	4.6 (2.4, 8.7)	<.001
Histologic pattern							
None	127 (58.5)	112 (78.3)	13 (48.1)	2 (8.7)	0	Control	
SRIF	54 (24.9)	30 (21.0)	12 (44.4)	9 (39.1)	3 (12.5)	4.3 (2.0, 9.5)	<.001
ILD (not UIP)	11 (5.1)	1 (0.7)	2 (7.4)	6 (26.1)	2 (8.3)	3.5 (0.96, 13)	.057
UIP	25 (11.5)	0	0	6 (26.1)	19 (79.2)	6.3 (2.6, 15.3)	<.001

Note.—Unless otherwise specified, data are numbers of patients, with percentages in parentheses. FEV₁ = forced expiratory volume in 1 second (percentage predicted for age, sex, and body height), FVC = forced vital capacity (percentage predicted for age, sex, and body height), ILA = interstitial lung abnormality, ILD = interstitial lung disease, IPF = idiopathic pulmonary fibrosis, MDD = multidisciplinary diagnosis (consensus diagnosis by the pulmonologist, the radiologist, and the pathologist), SRIF = smoking-related interstitial fibrosis, UIP = usual interstitial pneumonia.

* Data in parentheses are 95% confidence intervals.

[†] Data are means ± standard deviations.

[‡] As compared with wedge resection and other procedures (lobectomy and segmentectomy).

[§] As compared with stages I and II.

^{||} As compared with adenocarcinoma and others (squamous cell carcinoma [*n* = 31], large cell carcinoma [*n* = 6], pleomorphic carcinoma [*n* = 2], adenosquamous cell carcinoma [*n* = 1], sarcomatoid carcinoma [*n* = 1], and non-small cell lung cancer not otherwise specified [*n* = 2]).

Multivariable binary logistic regression analysis showed that GHNC-derived subpleural percentage fibrosis extent was significantly associated with the presence of a histologic UIP pattern. Subpleural fibrosis and fibroblastic foci are included in the criteria for defining a histologic UIP pattern (6). Thus, we considered that GHNC-CAD system would be useful for a detecting thin layer of subpleural fibrosis, which is easily missed by radiologists, suggesting a UIP pattern in these mild cases (15). It is notable that 84.6% (22 of 26) of patients who had a subpleural fibrosis extent of 27% or more showed disease progression at the follow-up CT examinations after 2 years. These findings suggest that subpleural fibrotic lesions may be an important factor in the progression of ILAs.

In the current study, 12 (25.5%) of 47 patients with ILAs were diagnosed as having SRIF. CT findings progressed in

six (13.6%) of 44 patients with SRIF after 2 years. Our study also demonstrated that the ILAs in the patients with unclassifiable interstitial pneumonia having airway-centered cystic lesions with fibrosis had progressed and that the cysts had enlarged in

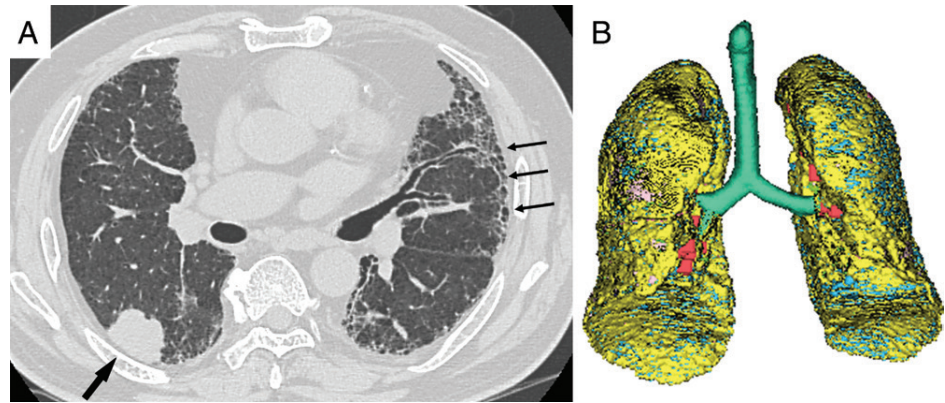


Figure 3: Images in 74-year-old male ex-smoker with the typical usual interstitial pneumonia (UIP) pattern and squamous cell carcinoma in the right lower lobe. He died of postoperative acute exacerbation of UIP. A, Initial axial CT image shows peripheral reticulation and honeycombing (thin arrows). Thick arrow = lung cancer. B, Three-dimensional Gaussian histogram normalized correlation (GHNC) image (front view) shows decreased lung volume, and the lung surface is covered with (yellow) H-pattern lesions. The subpleural percentage fibrosis extent measured by H-pattern volume in this subpleural lung area, within 2 mm under the pleura, was 59.3%. For GHNC images: pink = normal, dark blue = emphysema, light green = ground-glass opacity, light blue = reticulation, yellow = fibrosis, dark green = trachea and bronchi, orange = vessels.

Table 2: CT Findings and Their Association with Disease-free Survival according to Univariable Cox Regression Analysis

Finding	Total (n = 217)	No ILA (n = 143)	Equivocal ILA (n = 27)	ILA (n = 47)		Disease-free Survival	
				Not UIP (n = 23)	UIP (n = 24)	Hazard Ratio	P Value
Visual estimation of extent by radiologists							
Percentage normal	91.8 ± 12.9	97.2 ± 7.2	87.4 ± 17.4	81.1 ± 12.2	74.9 ± 11.3	0.95 (0.94, 0.97)	<.001
Percentage emphysema	4.0 ± 9.1	2.5 ± 7.0	9.2 ± 17.3	7.9 ± 7.8	4.1 ± 3.8	1.04 (1.01, 1.06)	<.001
Percentage consolidation	0.01 ± 0.14	0.0 ± 0.0	0.0 ± 0.0	0.0 ± 0.0	0.1 ± 0.1	2.4 (0.7, 8.3)	.167
Percentage GGO	1.0 ± 3.1	0.1 ± 0.4	0.9 ± 1.6	3.7 ± 6.0	3.8 ± 5.4	1.05 (0.99, 1.1)	.128
Percentage reticulation	2.8 ± 5.6	0.2 ± 0.7	2.4 ± 1.6	7.4 ± 5.8	14.6 ± 7.0	1.1 (1.06, 1.14)	<.001
Percentage honeycomb	0.3 ± 1.6	0.02 ± 0.21	0.02 ± 0.8	0.02 ± 0.9	2.6 ± 4.1	1.2 (1.1, 1.3)	<.001
Percentage fibrosis*	3.1 ± 6.3	0.2 ± 0.7	2.5 ± 1.6	7.4 ± 5.8	17.2 ± 7.8	1.1 (1.07, 1.13)	<.001
Percentage CT lung volume per GHNC [†]	94.0 ± 17.0	97.4 ± 16.6	94.3 ± 12.9	88.3 ± 16.1	78.7 ± 15.2	0.98 (0.96, 0.99)	.009
Extent per GHNC							
Percentage normal	84.1 ± 11.7	87.4 ± 8.2	81.4 ± 16.1	78.5 ± 12.0	72.9 ± 14.1	0.95 (0.94, 0.97)	<.001
Percentage emphysema	5.5 ± 9.6	4.8 ± 8.5	8.5 ± 15.8	7.4 ± 9.5	4.3 ± 5.1	1.04 (1.01, 1.06)	.006
Percentage GGO	4.6 ± 3.1	3.6 ± 2.1	4.7 ± 1.8	6.3 ± 3.6	8.3 ± 4.9	1.1 (1.08, 1.2)	<.001
Percentage consolidation	0.08 ± 0.10	0.05 ± 0.04	0.07 ± 0.05	0.09 ± 0.07	0.23 ± 0.21	36.6 (8.4, 160.3)	<.001
Percentage reticulation	1.3 ± 2.2	0.66 ± 0.8	1.3 ± 1.1	2.2 ± 2.9	4.5 ± 4.3	1.2 (1.09, 1.23)	<.001
Percentage fibrosis extent [‡]	4.5 ± 2.8	3.5 ± 0.9	4.1 ± 0.9	5.7 ± 2.9	9.9 ± 4.8	1.3 (1.19, 1.34)	<.001
Percentage subpleural fibrosis extent [§]	20.1 ± 9.0	16.3 ± 4.1	20.0 ± 4.5	25.2 ± 8.4	38.3 ± 10.4	1.1 (1.07, 1.12)	<.001

Note.—Data are means ± standard deviations. Data in parentheses are 95% confidence intervals. GGO = ground-glass opacity, GHNC = Gaussian histogram normalized correlation, ILA = interstitial lung abnormality, UIP = usual interstitial pneumonia.

* Sum of reticulation extent and honeycomb extent according to the radiologists.

[†] Total CT lung volume normalized for predicted total lung capacities.

[‡] H-pattern volume ratio in the whole lung.

[§] H2-pattern volume ratio in the 2-mm-width area of the lung surface.

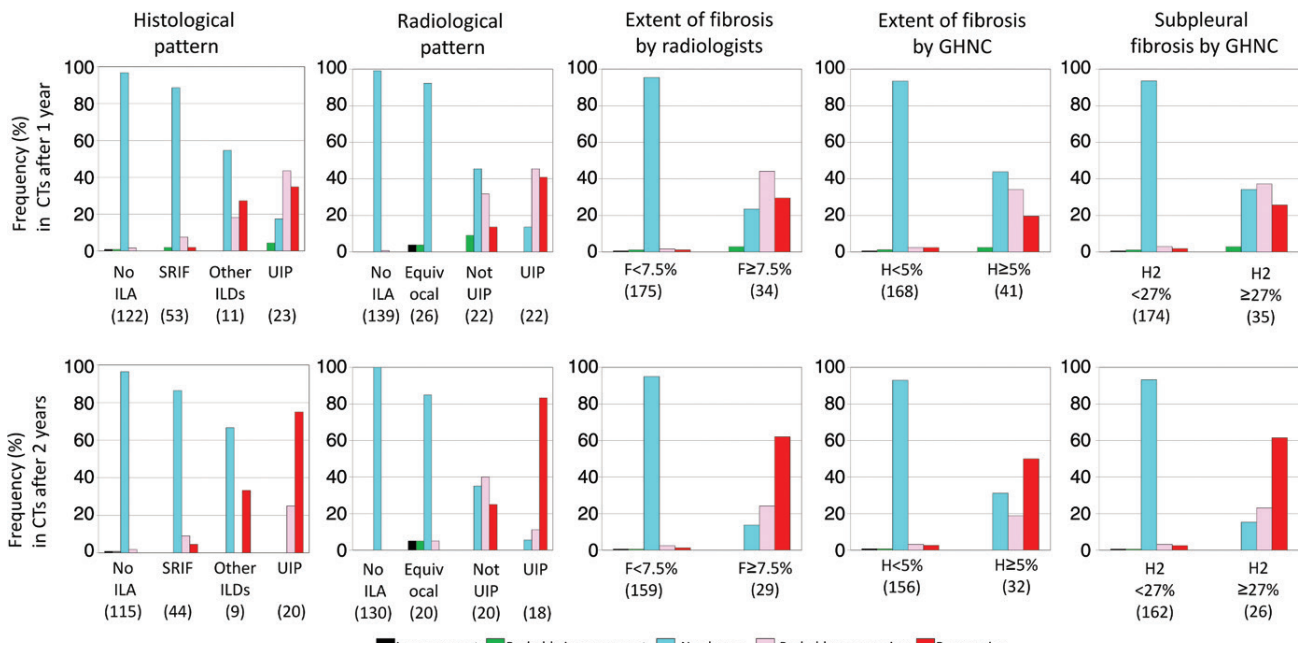


Figure 4: Bar graphs show changes in CT findings at follow-up CT examinations after 1 year (upper row) and after 2 years (lower row). Vertical axes show the percentage of patients with a change in CT findings (ie, improvement, probable improvement, no change, probable progression, and progression). Horizontal axes show the categories of histologic pattern, radiologic pattern, percentage fibrosis extent according to radiologists, percentage fibrosis extent according to a computer-aided detection (CAD) system with Gaussian histogram normalized correlation (GHNC), and subpleural fibrosis measured by the GHNC-CAD system. Numbers in parentheses = numbers of patients in each category. F = percentage fibrosis extent by the radiologists, H = percentage fibrosis extent by the GHNC-CAD system, H2 = subpleural percentage fibrosis extent by the GHNC-CAD system, ILA = interstitial lung abnormality, ILD = interstitial lung disease, SRIF = smoking-related interstitial fibrosis, UIP = usual interstitial pneumonia.

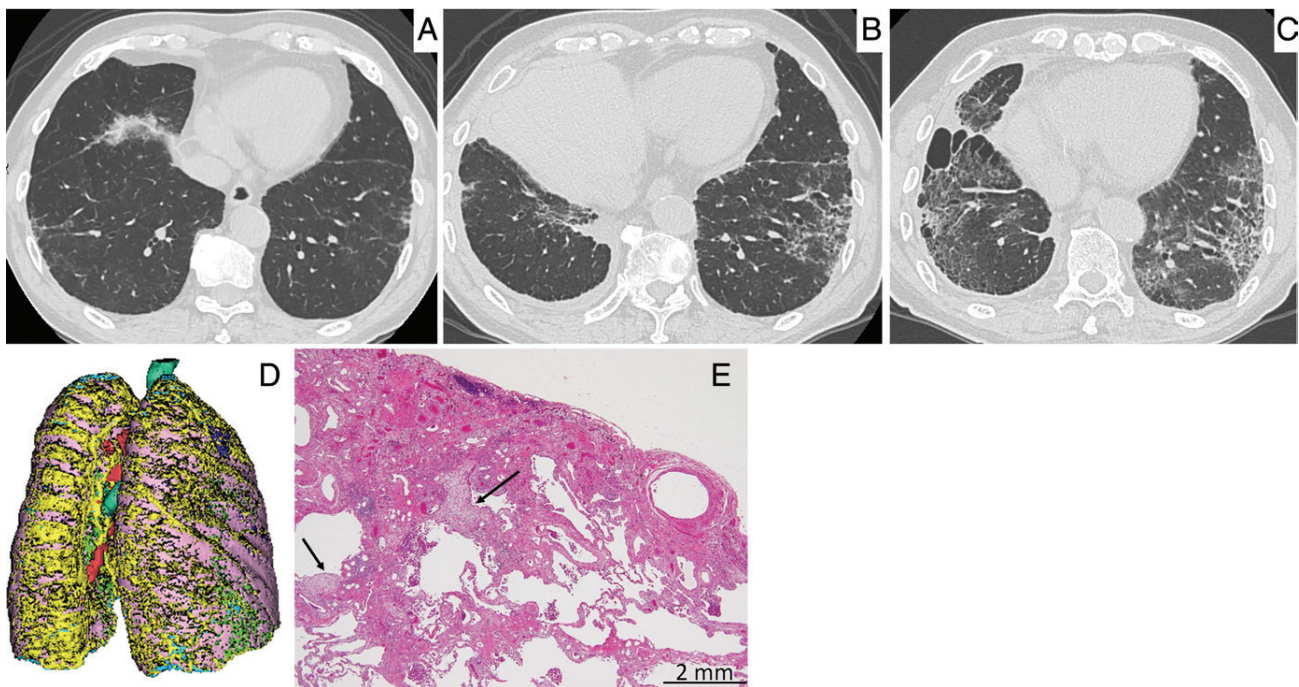


Figure 5: Images in 75-year-old male ex-smoker with idiopathic pulmonary fibrosis (based on a multidisciplinary diagnosis) and squamous cell carcinoma in the right lower lobe. *A*, Initial axial CT image shows reticulation but is indeterminate for usual interstitial pneumonia. *B*, Follow-up axial CT image at 1 year shows that reticulation has progressed. *C*, Axial CT image at 2.5 years reveals acute exacerbation and marked ground-glass opacities in the lungs bilaterally. This patient has been cured, is still alive and receiving home oxygen therapy 3.5 years after surgery, and is currently cancer free. *D*, On the three-dimensional Gaussian histogram normalized correlation (GHNC) image (back view) from the initial CT examination, a part of the lung surface is covered with (yellow) H-pattern lesions. The subpleural percentage fibrosis extent measured by GHNC was 27.3%. The colors of the GHNC image are the same as in Figure 3, *B*. *E*, Histologic specimen shows subpleural fibrosis with fibroblastic foci (arrows). (Hematoxylin-eosin stain; original magnification, $\times 20$; bar, 2 mm.)

Table 3: Results of Multivariable Logistic Regression Analysis of Clinical Factors and Fibrosis Extent according to the Computer-aided System for Evaluating the Association with the Existence of ILA and the UIP CT Pattern

Variable	Existence of Radiologic ILA		Existence of UIP CT Pattern	
	P Value	Odds Ratio	P Value	Odds Ratio
Age	.13	1.1 (0.99, 1.1)	.374	1.0 (0.95, 1.1)
Sex	.089	3.8 (0.8, 18)	.079	12.3 (0.75, 202)
Smoking index	.07	1.0 (0.99, 1.0)	.925	1.0 (0.98, 1.0)
Fibrosis extent per GHNC	<.001	3.1 (2.1, 4.7)	.001	2.0 (1.5, 2.6)

Note.—Data in parentheses are 95% confidence intervals. GHNC = Gaussian histogram normalized correlation, ILA = interstitial lung abnormality, UIP = usual interstitial pneumonia. Smoking index was determined by analyzing patient medical records. The existence of ILA and UIP were determined by the radiologists.

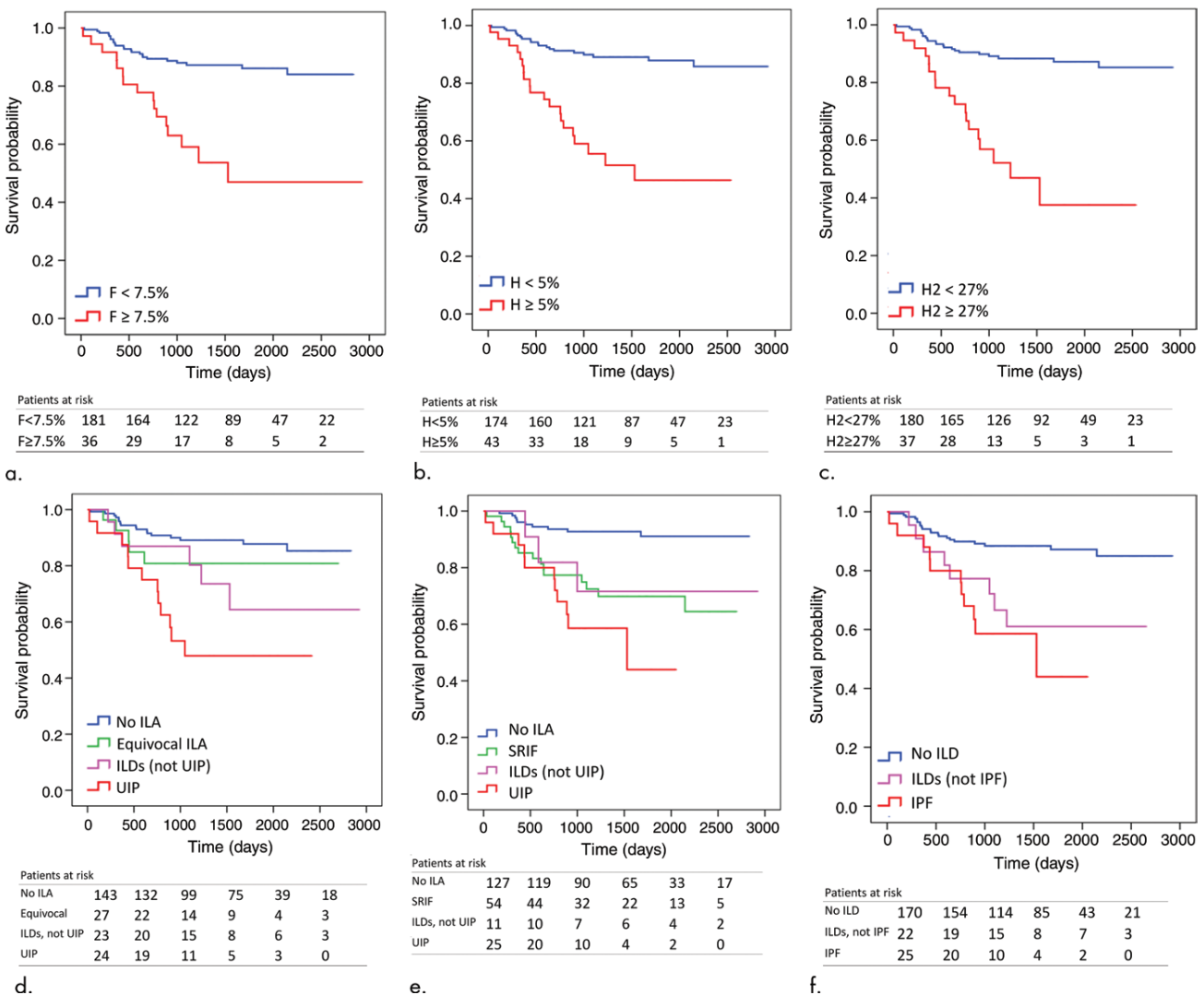


Figure 6: Graphs show Kaplan-Meier distribution of disease-free survival time. **(a)** Comparison between two groups on the basis of percentage of fibrosis extent according to the radiologists (F) (comparison of groups, $P < .001$). **(b)** Comparison between two groups on the basis of percentage of fibrosis extent according to the computer-aided detection (CAD) Gaussian histogram normalized correlation (GHNC) system (H) (comparison of groups, $P < .001$). **(c)** Comparison between two groups on the basis of percentage of subpleural fibrosis extent according to the GHNC-CAD system (H2) ($P < .001$). **(d)** Comparison between CT abnormalities determined by the radiologists. **(e)** Comparison between histologic findings. **(f)** Comparison between three groups on the basis of the multidisciplinary diagnosis (the consensus diagnosis by the pulmonologist, the radiologist, and the pathologist). ILA = interstitial lung abnormality, ILD = interstitial lung disease, IPF = idiopathic pulmonary fibrosis, SRIF = smoking-related interstitial fibrosis, UIP = usual interstitial pneumonia.

Table 4: Results of Multivariable Cox Regression Analysis of Disease-free Survival

Parameter	P Value	Hazard Ratio
Lung cancer stage	.005	3.4 (1.5, 7.9)
Age	.003	1.07 (1.02, 1.12)
Maximum cancer diameter	.741	1.01 (0.98, 1.03)
FEV ₁	.097	0.99 (0.98, 1.0)
Fibrosis extent according to GHNC system	.001	1.3 (1.1, 1.6)
Mean fibrosis extent determined by radiologists	.421	0.97 (0.90, 1.05)

Note.—Data in parentheses are 95% confidence intervals. FEV₁ = forced expiratory volume in 1 second (percentage predicted for age, sex, and body height), GHNC = Gaussian histogram normalized correlation.

the follow-up CT studies (33). It is difficult to distinguish “early” UIP from other types of fibrosis at preoperative CT (34). Larger normal lung volume ratio was associated with better DFS (hazard ratio, 0.95; $P < .001$), and patients without ILA showed better prognosis. We believe normal lung volume is also important for preoperative assessment.

The lower sensitivity of percentage fibrosis extent according to the GHNC-CAD system in determining the UIP CT pattern compared with that according to the radiologists may be attributed to the misclassification of normal peripheral structures as fibrotic lesions by the GHNC-CAD system. The GHNC-CAD system counted a part of reticulation surrounding the traction bronchiectasis/bronchiolectasis as fibrosis. The radiologist-assessed percentage fibrosis extent, including all the reticulation, was larger than that according to the CAD system in patients with ILAs. This explains the higher cutoff values for radiologist-assessed percentage fibrosis extent.

This retrospective study had several limitations. First, it was performed in a single center, and the study population was too small to allow us to assess multiple variables adequately. We could not conclude that the GHNC-CAD analysis was superior to radiologists’ scoring. Second, we used CT images obtained from a single vendor’s hardware and software platform; this limits the generalizability of these results. However, in a previous report, the GHNC-CAD system worked well with three different manufacturers of CT scanners (35). We evaluated surgical specimens resected for lung tumors in the same lobe. Thus, this evaluation was limited to the histologic findings of ILAs in the specimen, and the rest of the lung was not sampled. A prospective multicenter study with a larger number of patients will be necessary to overcome these many limitations.

In conclusion, the volume ratio of fibrosis at preoperative CT, as measured by using a computer-aided detection (CAD) system, was an independent predictor of lower disease-free survival in patients with lung cancer. CAD using the Gaussian histogram normalized correlation system provided prognostic information for treating patients with lung cancer.

Author contributions: Guarantors of integrity of entire study, T.I., A.Y.; study concepts/study design or data acquisition or data analysis/interpretation, all authors;

manuscript drafting or manuscript revision for important intellectual content, all authors; approval of final version of submitted manuscript, all authors; agrees to ensure any questions related to the work are appropriately resolved, all authors; literature research, T.I., T.T., M.T., A.Y.; clinical studies, T.I., T.T., S.M., T.B., T.O., M.T., A.Y.; experimental studies, T.I., K.O., T.F., M.T., A.Y.; statistical analysis, T.I., M.T., A.Y.; and manuscript editing, T.I., K.O., T.T., T.O., M.T., A.Y.

Disclosures of Conflicts of Interest: T.I. Activities related to the present article: disclosed no relevant relationships. Activities not related to the present article: is a consultant for Ono Pharmaceutical; is on the speakers bureaus of Canon Medical Systems, Fuji Film, Boehringer Ingelheim, and Shionogi; institution has patent (2016-39752) pending. Other relationships: disclosed no relevant relationships. K.O. disclosed no relevant relationships. T.T. disclosed no relevant relationships. T.F. disclosed no relevant relationships. S.M. disclosed no relevant relationships. T.B. Activities related to the present article: disclosed no relevant relationships. Activities not related to the present article: has been paid for expert testimony by AstraZeneca, Daiichi Sankyo, Ono Pharmaceutical, and Bristol Myers Squibb; is on the speakers bureaus of AstraZeneca, Boston Scientific Japan, Nippon Boehringer Ingelheim, Toray Industries, Shionogi, Astellas Pharma, AMCO, Asahi Kasei Pharma, Bristol Myers Squibb, and Taiho Pharmaceutical; has been paid for development of educational presentations by MSD; has received travel expenses from Kyorin Pharmaceutical. Other relationships: disclosed no relevant relationships. T.O. Activities related to the present article: disclosed no relevant relationships. Activities not related to the present article: is on the advisory boards of Nippon Boehringer Ingelheim and Asahi Kasei; institution has grants or grants pending from Nippon Boehringer Ingelheim; is on the speakers bureaus of Nippon Boehringer Ingelheim, Shionogi, and Eisai; has received payment for manuscript preparation from Nippon Boehringer Ingelheim. Other relationships: disclosed no relevant relationships. M.T. disclosed no relevant relationships. A.Y. disclosed no relevant relationships.

References

- Hatabu H, Hunninghake GM, Lynch DA. Interstitial lung abnormality: recognition and perspectives. *Radiology* 2019;291(1):1–3.
- Washko GR, Hunninghake GM, Fernandez IE, et al. Lung volumes and emphysema in smokers with interstitial lung abnormalities. *N Engl J Med* 2011;364(10):897–906.
- Jin GY, Lynch D, Chawla A, et al. Interstitial lung abnormalities in a CT lung cancer screening population: prevalence and progression rate. *Radiology* 2013;268(2):563–571.
- Putman RK, Hatabu H, Araki T, et al. Association between interstitial lung abnormalities and all-cause mortality. *JAMA* 2016;315(7):672–681.
- Tsushima K, Sone S, Yoshikawa S, Yokoyama T, Suzuki T, Kubo K. The radiological patterns of interstitial change at an early phase: over a 4-year follow-up. *Respir Med* 2010;104(11):1712–1721.
- Miller ER, Putman RK, Vivero M, et al. Histopathology of interstitial lung abnormalities in the context of lung nodule resections. *Am J Respir Crit Care Med* 2018;197(7):955–958.
- Nishino M, Cardarella S, Dahlberg SE, et al. Interstitial lung abnormalities in treatment-naïve advanced non-small-cell lung cancer patients are associated with shorter survival. *Eur J Radiol* 2015;84(5):998–1004.
- Omori T, Tajiri M, Baba T, et al. Pulmonary resection for lung cancer in patients with idiopathic interstitial pneumonia. *Ann Thorac Surg* 2015;100(3):954–960.
- Saito Y, Kawai Y, Takahashi N, et al. Survival after surgery for pathologic stage IA non-small cell lung cancer associated with idiopathic pulmonary fibrosis. *Ann Thorac Surg* 2011;92(5):1812–1817.
- Usui K, Tanai C, Tanaka Y, Noda H, Ishihara T. The prevalence of pulmonary fibrosis combined with emphysema in patients with lung cancer. *Respirology* 2011;16(2):326–331.
- Iwasawa T, Asakura A, Sakai F, et al. Assessment of prognosis of patients with idiopathic pulmonary fibrosis by computer-aided analysis of CT images. *J Thorac Imaging* 2009;24(3):216–222.
- Maldonado F, Moua T, Rajagopalan S, et al. Automated quantification of radiological patterns predicts survival in idiopathic pulmonary fibrosis. *Eur Respir J* 2014;43(1):204–212.
- Jacob J, Bartholmai BJ, Rajagopalan S, et al. Mortality prediction in idiopathic pulmonary fibrosis: evaluation of computer-based CT analysis with conventional severity measures. *Eur Respir J* 2017;49(1):1601011.
- Ash SY, Harmouche R, Ross JC, et al. Interstitial features at chest CT enhance the deleterious effects of emphysema in the COPDGene cohort. *Radiology* 2018;288(2):600–609.
- Iwasawa T, Takemura T, Okudera K, et al. The importance of subpleural fibrosis in the prognosis of patients with idiopathic interstitial pneumonias. *Eur J Radiol* 2017;90:106–113.
- Detterbeck FC, Boffa DJ, Kim AW, Tanoue LT. The eighth edition lung cancer stage classification. *Chest* 2017;151(1):193–203.
- Sumikawa H, Johkoh T, Fujimoto K, et al. Pathologically proved nonspecific interstitial pneumonia: CT pattern analysis as compared with usual interstitial pneumonia CT pattern. *Radiology* 2014;272(2):549–556.
- Lynch DA, Sverzellati N, Travis WD, et al. Diagnostic criteria for idiopathic pulmonary fibrosis: a Fleischner Society White Paper. *Lancet Respir Med* 2018;6(2):138–153.
- Araki T, Putman RK, Hatabu H, et al. Development and progression of interstitial lung abnormalities in the Framingham Heart Study. *Am J Respir Crit Care Med* 2016;194(12):1514–1522.

20. Iwao Y, Gotoh T, Kagei S, Iwasawa T, MGS. T. Integrated lung field segmentation of injured region with anatomical structure analysis by failure–recovery algorithm from chest CT images. *Biomed Signal Process Control* 2014;12:28–38.
21. Iwasawa T, Iwao Y, Takemura T, et al. Extraction of the subpleural lung region from computed tomography images to detect interstitial lung disease. *Jpn J Radiol* 2017;35(11):681–688.
22. Travis WD, Costabel U, Hansell DM, et al. An official American Thoracic Society/European Respiratory Society statement: update of the international multidisciplinary classification of the idiopathic interstitial pneumonias. *Am J Respir Crit Care Med* 2013;188(6):733–748.
23. Raghu G, Collard HR, Egan JJ, et al. An official ATS/ERS/JRS/ALAT statement: idiopathic pulmonary fibrosis: evidence-based guidelines for diagnosis and management. *Am J Respir Crit Care Med* 2011;183(6):788–824.
24. Katzenstein AL, Mukhopadhyay S, Zanardi C, Dexter E. Clinically occult interstitial fibrosis in smokers: classification and significance of a surprisingly common finding in lobectomy specimens. *Hum Pathol* 2010;41(3):316–325.
25. Raghu G, Remy-Jardin M, Myers JL, et al. Diagnosis of idiopathic pulmonary fibrosis: an official ATS/ERS/JRS/ALAT Clinical Practice Guideline. *Am J Respir Crit Care Med* 2018;198(5):e44–e68.
26. Kundel HL, Polansky M. Measurement of observer agreement. *Radiology* 2003;228(2):303–308.
27. Miyajima M, Watanabe A, Sato T, et al. What factors determine the survival of patients with an acute exacerbation of interstitial lung disease after lung cancer resection? *Surg Today* 2018;48(4):404–415.
28. Kinoshita T, Azuma K, Sasada T, et al. Chemotherapy for non-small cell lung cancer complicated by idiopathic interstitial pneumonia. *Oncol Lett* 2012;4(3):477–482.
29. Kobayashi H, Naito T, Omae K, et al. Impact of interstitial lung disease classification on the development of acute exacerbation of interstitial lung disease and prognosis in patients with stage III non-small-cell lung cancer and interstitial lung disease treated with chemoradiotherapy. *J Cancer* 2018;9(11):2054–2060.
30. Kanaji N, Tadokoro A, Kita N, et al. Impact of idiopathic pulmonary fibrosis on advanced non-small cell lung cancer survival. *J Cancer Res Clin Oncol* 2016;142(8):1855–1865.
31. Sverzellati N, Guerci L, Randi G, et al. Interstitial lung diseases in a lung cancer screening trial. *Eur Respir J* 2011;38(2):392–400.
32. Tzouveleakis A, Spagnolo P, Bonella F, et al. Patients with IPF and lung cancer: diagnosis and management. *Lancet Respir Med* 2018;6(2):86–88.
33. Iwasawa T, Takemura T, Ogura T. Smoking-related lung abnormalities on computed tomography images: comparison with pathological findings. *Jpn J Radiol* 2018;36(3):165–180.
34. Kawabata Y, Hoshi E, Murai K, et al. Smoking-related changes in the background lung of specimens resected for lung cancer: a semiquantitative study with correlation to postoperative course. *Histopathology* 2008;53(6):707–714.
35. Iwasawa T, Kanauchi T, Hoshi T, et al. Multicenter study of quantitative computed tomography analysis using a computer-aided three-dimensional system in patients with idiopathic pulmonary fibrosis. *Jpn J Radiol* 2016;34(1):16–27.